Available online at www.sciencedirect.com
SCIENCE DIRECT®
Journal of Chemical Neuroanatomy 30 (2005) 71–81
Journal of CHEMICAL NEUROANATOMY
www.elsevier.com/locate/jchemneu

Neuropil reactivity, distribution and morphology of NADPH diaphorase type I neurons in the barrel cortex of the adult mouse

Marco Aurélio M. Freire [a], João G. Franca [b], Cristovam W. Picanço-Diniz [a], Antônio Pereira Jr.[a,*]

[a] *Laboratory of Functional Neuroanatomy, Department of Morphology, Biological Sciences Building, Federal University of Pará, 66075-900 Belém, PA, Brazil*
[b] *Institute of Biophysics Carlos Chagas Filho, Federal University of Rio de Janeiro, Rio de Janeiro, RJ, Brazil*

Received 6 October 2004; received in revised form 11 January 2005; accepted 25 April 2005
Available online 5 July 2005

Abstract

The mouse, like a few other rodent and marsupial species, displays a striking modular architecture in its primary somatosensory cortex (SI). These modules, known as barrels, are mostly defined by the peculiar arrangement of granule cells and thalamic axons in layer IV. In the present work, we studied both the distribution and morphology of neurons stained for NADPH diaphorase (NADPH-d) and neuropil reactivity in the posteromedial barrel subfield (PMBSF), which represents the mystacial whiskers. We then compared our results with previous descriptions of NADPH-d distribution in both neonatal and young mice. We found two types of neurons in the PMBSF: type I neurons, which have large cell bodies and are heavily stained by the NADPH-d reaction; and type II neurons, characterized by relatively small and poorly stained cell bodies. The distribution of type I cells in the PMBSF was not homogenous, with cells tending to concentrate in septa between barrels. Moreover, the cells found in septal region possess both a larger and more complex dendritic arborization than cells located inside barrels. Our findings are at variance with results from other groups that reported both an absence of type II cells and a homogeneous distribution of type I cells in the PMBSF of young animals. In addition, our results show a distribution of type I cells which is very similar to that previously described for the rat's barrel field.

Keywords: Somatosensory cortex; Barrel field; Nitric oxide; Interneurons; Morphometric analysis; Fractal dimension; Rodent

1. Introduction

The primary somatosensory cortex (SI) of the mouse is composed by a mosaic of granule cell aggregates shaped like barrels (Woolsey and van der Loos, 1970; Welker and Woolsey, 1974; Woolsey et al., 1975). The barrels have two distinct regions, a cell-sparse hollow and a cell-rich wall, both easily visualized in tangential sections of the brain stained by the Nissl technique (see Woolsey and van der Loos, 1970). The barrel field corresponds to a complete topographical representation of the contralateral cutaneous sensory periphery (for review see Rice, 1995). The largest barrels are located in the posteromedial barrel subfield (PMBSF) and are individually related to the large mystacial whiskers of the contralateral snout (van der Loos and Woolsey, 1973; Woolsey et al., 1975). Other body parts represented in the barrel field, such as the lower lip and the paws, can also be easily identified in tangential sections of the brain (Wallace, 1987). Each barrel is separated from its neighbors by myelin-rich septa (for a review see Rice, 1995). In the mouse, similar to other small rodents (Woolsey et al., 1975; Franca and Volchan, 1995), and some marsupials (Weller, 1993), barrels can also be visualized by revealing the distribution of enzymes such as cytochrome oxidase (CO) (Wong-Riley and Welt, 1980), succinic dehydrogenase (SDH) (Wallace, 1987), and

* Corresponding author. Present address: Duke University Medical Center, Department of Neurobiology, Box 3209, Durham, NC 27710, USA. Tel.: +55 91 3183 1741; fax: +55 91 3183 1741.
E-mail address: freire.m@uol.com.br (A. Pereira Jr.).

0891-0618/$ – see front matter
doi:10.1016/j.jchemneu.2005.04.006

nicotinamide adenine dinucleotide phosphate diaphorase (NADPH-d) (Pereira Jr. et al., 2000).

NADPH-d, in the neocortex, is usually associated with GABAergic neurons (Valtschanoff et al., 1993) and has drawn interest since the demonstration that neurons containing this enzyme are resistant to injury mediated by many factors lethal to other cell groups (Thomas and Pearse, 1964; Ferrante et al., 1985), such as the excessive concentration of excitatory amino acids (Koh et al., 1986), malnutrition (Picanço-Diniz et al., 1998) and intoxication by heavy metals (Oliveira et al., 1998). NADPH-d has also been characterized as a nitric oxide synthase (NOS) and has been used to identify neurons that express the neurotransmitter nitric oxide (NO) (Dawson et al., 1991; Hope et al., 1991), a gas which readily diffuses through both lipid and aqueous media and has a half-life of a few seconds (Vincent, 1994). During postnatal development of the nervous system, NO is involved in many critical processes, such as the establishment of synapses in the optic *tectum* (Ernst et al., 1999), differentiation of motor neurons in the spinal cord (Kalb and Agostini, 1993) and granule cell migration in the cerebellum (Tanaka et al., 1994). In the adult brain, NO continues to play important roles in the regulation of cerebral blood flow (Estrada and DeFelipe, 1998), long term potentiation (Bohme et al., 1991), neurogenesis (Moreno-Lopez et al., 2000), synaptic plasticity (Hölscher, 1997), and programmed cell death (Estevez et al., 1998). In knockout studies, Nelson et al. (1995) have shown that adult mice with targeted disruption on NOS display grossly altered behavior. On the other hand, excessive concentrations of NO in the central nervous system has been shown to be harmful, probably due to its oxidative properties (Lipton et al., 1993).

The distribution and histochemical characterization of NADPH-d neurons have been evaluated before in the brain of several mammalian species (Sandell, 1986; Vincent and Kimura, 1992; Valtschanoff et al., 1993; Hashikawa et al., 1994; Kubota and Kawaguchi, 1994; Volchan and Franca, 1994; Yan et al., 1996; Bidmon et al., 1997; Franca et al., 1997, 2000; Yan and Garey, 1997; Oermann et al., 1999; Freire et al., 2004). In the mouse barrel field, the distribution of NADPH-d was described before by Mitrovic and Schachner (1996). These authors, however, analyzed the cortical distribution of NADPH-d neurons only from day of birth (P0) up to the second postnatal week of brain development (P15), leaving unaccounted the distribution of NADPH-d cells in the adult barrel field. In the present study, we filled in this gap by examining the distribution pattern of NADPH-d neurons in both tangential and coronal sections of the barrel cortex of adult mice, with special emphasis on the cytoarchitectonic subdivisions within SI. Also, we present quantitative evidence that NADPH-d neurons inside barrels are morphologically different from the ones in barrel septa in terms of dendritic arbor coverage and complexity (i.e., fractal dimension).

2. Materials and methods

2.1. Animals and tissue preparation

Eleven adult albino mice (*Mus musculus)* were used in the present study (Table 1). All efforts were made to avoid animal suffering and distress and to reduce the number of animals used. All experimental procedures were carried out in accordance to the NIH guidelines (Guide for the care and use of laboratory animals).

Animals were deeply anaesthetized with a mixture of xylazine chloridrate and ketamine chloridrate (4.0 and 46 mg/kg, i.m., respectively) and perfused through the left ventricle with 200 ml of 0.9% saline solution, followed by 150–300 ml of 4% paraformaldehyde in 0.1 M sodium phosphate buffer (PB). After craniotomy the brains were dissected, and some of them ($n = 8$) had the cortical hemispheres flattened between two glass slides and immersed in 0.1 M PB for about 10 h. The brains were sectioned either tangentially or coronally ($n = 3$) into 100 μm thick sections with a vibratome (Pelco International, Series 1000). Some tangential hemispheres ($n = 4$) were cut at 50 μm thick sections for NOS immunohistochemistry (see Table 1).

2.2. Histochemistry

Brain sections were collected in 0.1 M PB washed three times and incubated free-floating in a medium containing 0.6% malic acid, 0.03% nitroblue tetrazolium, 1% dimethylsulfoxide, 0.03% manganese chloride, 0.5% β-NADP and 1.5–3% Triton X-100 in 0.1 M Tris buffer, pH 8.0 (modified from Scherer-Singler et al., 1983). The NADPH-d histochemical reaction was continuously monitored to prevent overstaining. Sections were incubated for the same time and in the same solution for every animal. The reaction was usually interrupted after 3–4 h by rinsing sections in PB (pH 7.4). Sections were mounted onto gelatin-coated glass slides and left to air-dry overnight.

CO histochemistry was used as a standard for the intrinsic organization of the barrel field (Wong-Riley and Welt, 1980). CO activity was revealed in a series of adjacent coronal sections incubated in a solution containing 0.05% diaminobenzidine (DAB), 0.03% cytochrome *c* and 0.02% catalase in 0.1 M PB (Wong-Riley, 1979). The reaction was monitored every 30 min in order to avoid overstaining. The duration of the incubation ranged from 6 to 7 h and was

Table 1
Summary of animals and procedures utilized

Number of animals	Section plan	Thickness (μm)	Histology
4	Tangential	100	NADPH-d
2	Tangential	50	NADPH-d/NOS
3	Coronal	100	NADPH-d/CO/Nissl
2	Tangential	100	Nissl

interrupted by rinsing the sections in 0.1 M PB (pH 7.4). All reagents were purchased from Sigma Company, USA.

2.3. Immunohistochemistry

NOS immunohistochemistry was performed in some sections previously reacted for NADPH-d. Sections were washed three times in a medium containing 0.05% 0.1 M phosphate buffer saline-Tween (PBS-T) and incubated in 10% normal goat serum in PBS for 1 h. After that, sections were incubated in mouse anti-NOS primary antibody (dilution at 1:150 in PBS, Serotec, UK) for 48 h at 10 °C, washed three times in PBS-T and incubated with a biotinylated goat anti-mouse secondary antibody (dilution at 1:200 in PBS, Serotec) for 1 h, washed three times in PBS-T, and then incubated in avidin-biotin-peroxidase solution (Vectastain Standard ABC kit, Vector Laboratories, USA) for 1 h. In this study, we used the DAB/nickel method for revealing NOS antibody in NADPH-d labeled tissue, as described by Picanço-Diniz et al. (2004), with the difference that the NADPH-d reaction was performed before the immunohistochemistry procedure, yielding to a lighter reaction product than if the immunohistochemistry is performed first. This protocol (Picanço-Diniz et al., 2004) also ensures a lighter reaction product with better visualization of double labeling because a smaller amount of nickel is used, as compared to regular DAB/nickel protocol (Shu et al., 1988). In order to certify the specificity of the NOS-labeling, normal serum rather the primary antibody was used in some sections.

Some sections were counterstained with cresyl violet (Nissl stain). Finally, all sections were dehydrated and coverslipped with Entellan (Merck, Germany).

2.4. Quantitative analysis

The barrel field was drawn from tangential sections using the software *Neurolucida* (MicroBrightField Inc., USA). The areas of both the entire PMBSF and individual barrels were measured using the software *Scion Image for Windows*, version Beta 4.0.2 (Scion Corporation, USA). In order to determine the PMBSF total area a continuous line was drawn connecting the outermost limit of the ''external'' PMBSF barrels of this subfield (see boxes in Fig. 6). Individual barrel areas were summed up in order to calculate the total area occupied by barrels. The value of the septal area was then obtained by simply subtracting the area occupied by the individual barrels from the total PMBSF area.

For the quantitative analysis of the distribution of NADPH-d neurons we used tangential reconstructions from cortical middle layers ($n = 9$ hemispheres from five animals, three drawings per hemisphere). For each animal, three 100 μm thick tangential sections were reconstructed and superimposed using the blood vessels as landmarks. This procedure allowed the complete reconstruction of the PMBSF, since the barrels measure about 300 μm across the middle layers (Zilles and Wree, 1985).

The position of NADPH-d cells relative to both septa and barrels were depicted on the drawings. Estimates of cell number were obtained for both subregions. Two groups of values were obtained, by comparing distribution in barrel's septa versus barrel's hollows. A cell was considered to belong to either a septum or a barrel only if its cell body was completely enclosed by that structure. Borderline cells were not considered.

Type I NADPH-d neurons located both in septa and barrels ($n = 30$ for each region) were reconstructed with *Neurolucida* using a 60× oil-objective. The main criterion to choose a cell was the presence of a fairly complete dendritic arborization (cells whose dendrites seemed to be cut were not included in the quantification). *Scion Image* was used to obtain areal measurements for both cell bodies and dendritic arborization, in μm^2. We also used *Scion Image* to calculate the bi-dimensional fractal dimension (D) of the dendritic field of these cells (Caserta et al., 1995; see Jelinek and Fernandez, 2001 for review). We chose to adopt the dilation method, which has been used to determine the D in other neuronal populations (Jelinek and Elston, 2001, 2003). This method determines the D for each cell by overlaying the original dendritic arborization with successively larger pixel arrays (dilation) and computing the relationship between the total dendritic length of each successive image with respect to the increasing width of the array (Jelinek and Fernandez, 1998). The dilation method is deemed more sensitive to determine D since it incorporates all points in the dendritic arborization, unlike other methods such as mass-radius or box counting (see Jelinek and Fernandez, 1998, 2001 for details).

Quantitative data were compared using a two-tailed Student's t-test. The values obtained were referred as means ± standard error (SEM). Statistical significance was accepted at the 95% confidence level ($^{*}p < 0.05$); high significance was adopted at 99% confidence level ($^{**}p < 0.01$).

3. Results

As previously reported elsewhere (Pereira Jr. et al., 2000), the NADPH-d histochemistry reveals the entire barrel field of the adult mouse in a pattern similar to that obtained with other histochemical methods, such as succinic dehydrogenase (SDH) (Wallace, 1987) and cytochrome oxidase (CO) (Wong-Riley and Welt, 1980).

Two types of reactive neurons were readily identified in mouse SI: type I and type II cells (Lüth et al., 1994). Both corresponded to non-pyramidal neurons in which the labeling patterns were very different from each other (Fig. 1). Type I neurons were more intensely labeled and also had a cell body much larger than type II neurons. Type II neurons had a ghost-like appearance, when compared to type

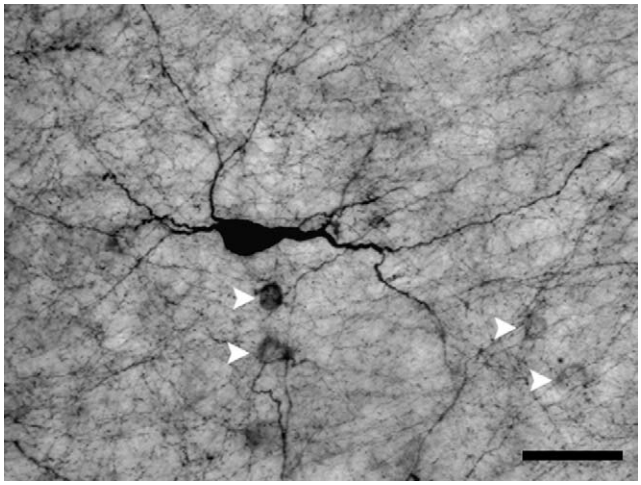

Fig. 1. NADPH-d cell types I and II in the SI cortex. Type I neurons have considerably larger cell bodies, have a more exuberant dendritic field and stain more heavily than type II neurons (arrowheads). Scale bar: 30 μm.

I cells, and, due to their small diameter, could be mistaken for glial cells, especially when viewed at low magnifications. Another distinctive feature is that the dendritic tree of type II neurons was poorly labeled or not labeled at all.

The overall morphology of type I neurons was quite diverse, including multipolar, stellate, and bipolar cells, which possessed dendrites with a sharp tapering profile (Fig. 1). These morphological differences follow the general pattern observed for other populations of inhibitory interneurons (Lorente de Nó, 1992; see DeFelipe, 1997 for review). In respect to type II neuron morphology, it was rather difficult to reliably classify them due to their diminished body size and lack of most dendritic detail (see Fig. 1).

3.1. Areal measurements and quantitative analysis of type I neuronal morphology

The average total area of the PMBSF was $3.16 \pm 0.34\ mm^2$. The average areas occupied by either barrels or septa were markedly similar in size (barrels: $1.62 \pm 0.11\ mm^2$; septa: $1.54 \pm 0.10\ mm^2$; $p > 0.05$) (Fig. 2). The relative proportion of PMBSF area occupied by each of these structures was similar to that reported for the adult rat (Franca, 1999; Freire et al., 2004). This result is in disagreement with a previous description in the rat (Riddle et al., 1992), which points to a larger area occupied by barrels than by septa. Such discrepancy can be explained by a difference in the definition of the total PMBSF area. Riddle et al. (1992) calculated this area using the centroids of barrels, leaving thus unaccounted a substantial portion of the septa lying in-between the outermost barrels of PMBSF.

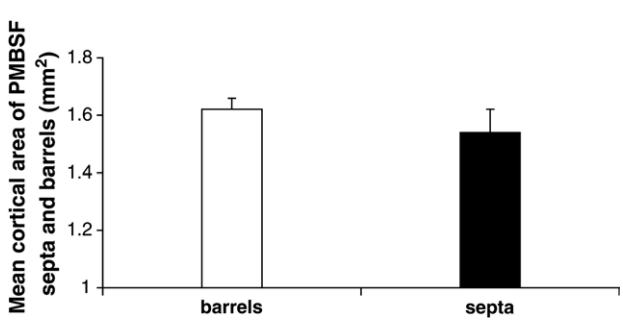

Fig. 2. Cortical area occupied by either barrels and septa in the PMBSF. There was no significant difference between the areas occupied by the two subcompartments ($p > 0.05$; Student's *t*-test).

In a qualitative inspection, it was possible to notice that there is a large diversity in both cell body morphology and dendritic arborization between septa and barrel neurons (Fig. 3A). However, there was not a significant difference in cell bodies' areas between these two regions (septa: $103.2 \pm 22.4\ \mu m^2$; barrels: $105.3 \pm 22.3\ \mu m^2$; $p > 0.05$) (Fig. 4A). On the other hand, the measurements for the dendritic fields revealed a significant difference among them, with the septal neurons having a larger dendritic

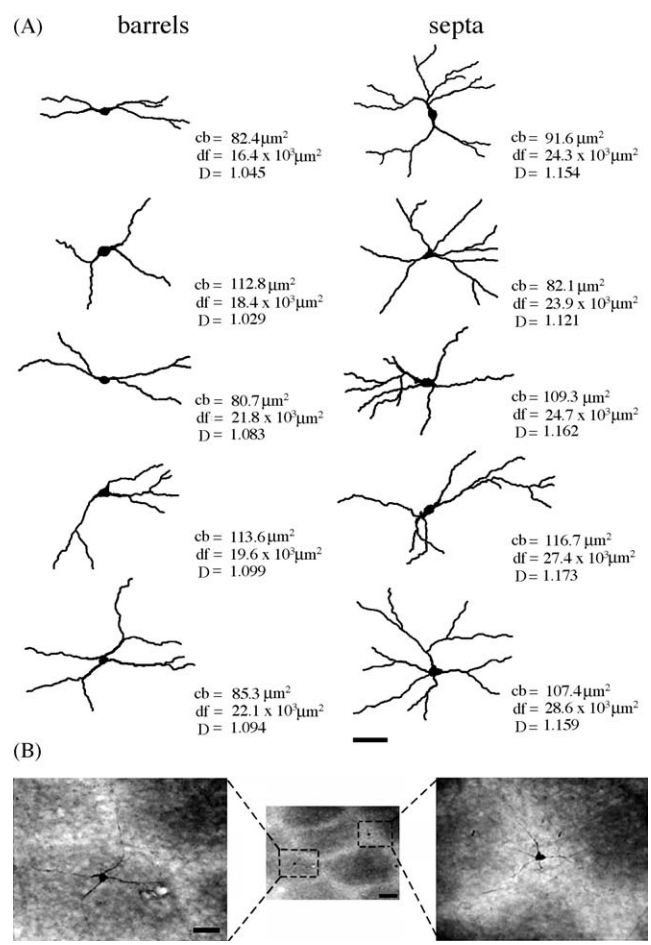

Fig. 3. Reconstructions of NADPH-d type I neurons in both barrels and septa. The septal cells possess a more elaborated dendritic arborization than those inside barrels (A). Dendritic arbors were usually not restricted to the architectonic limits of these structures (B) (the reconstruction of the cells depicted here are in the lower part of A). Legends: cb: cell body; df: dendritic field; *D*: fractal dimension. Scale bars: 30 μm in (A) and enlargements of (B); 100 μm in low magnification of (B).

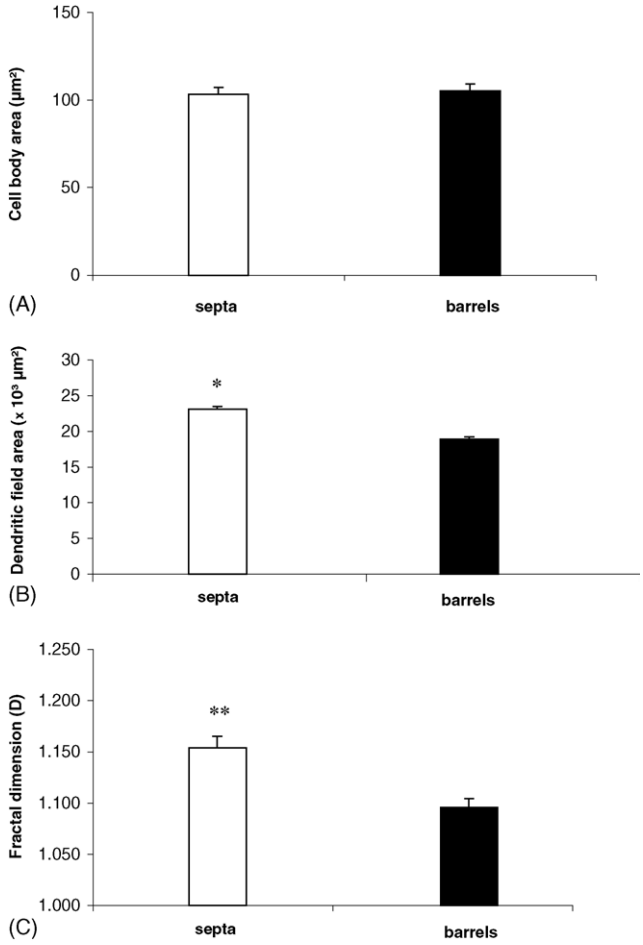

Fig. 4. Comparative morphometry of NADPH-d type I neurons in barrels and septa. There was no significant difference in cell body areas located in either subregion ($p > 0.05$) (A). On the other hand, both dendritic field areas (B) and fractal dimensions (C) of cells in septa are significantly higher than those in barrels ($^{*}p < 0.05$ and $^{**}p < 0.01$, respectively; Student's *t*-test).

coverage (septa: $22.3 \times 10^3 \pm 2.3 \times 10^3$ µm^2; barrels: $19.3 \times 10^3 \pm 1.7 \times 10^3$ µm^2; $p < 0.05$) (Fig. 4B). The values of fractal dimension for the dendritic fields in each region also differed significantly, signaling that septal neurons have more complex dendritic fields (septa: 1.154 ± 0.063; barrels: 1.096 ± 0.046; $p < 0.01$) (Fig. 4C). Besides, both septum and barrel cells could send their dendrites beyond the cytoarchitectonic limits of these structures (Fig. 3B).

3.2. Laminar and tangential NADPH-d distribution in the PMBSF neuropil

In a coronal view, the NADPH-d neuropil reactivity provided a clear picture of the layered arrangement of the SI cortex (Fig. 5A), similar to what has been described before for CO (Wong-Riley and Welt, 1980). Layer I appeared as a band of moderate reaction. In layers II and III, however, the diffuse histochemical product displayed an elevated reactivity evenly distributed between these two layers, making it rather difficult to depict the limit between them. In layer IV, NADPH-d activity was heterogeneously distributed, revealing round patches of intense reactivity (barrels) separated from each other by less reactive regions (septa). Layer V is characterized as a region of low reactivity. Enzymatic reactivity increased again in layer VI, making it rather easy to identify the limit between this layer and the white matter (Fig. 5A). In layer VI we also could discern some patches of reactivity laid in close register with the layer IV barrels, though fainter (Fig. 5A). These patches were not visible either with Nissl or CO histochemistry. In addition, layer VI seems to be subdivided into two regions, a more reactive upper sublayer (where the fainter patches are seen) and a less reactive lower sublayer, as cytoarchitectonically described by Lorente de Nó (1992) (see also Fig. 5B). In the white matter, the enzymatic reactivity was more homogeneous, and it was considerably lower than that seen in any other cortical layer (Fig. 5A). The limits amongst layers provided by the NADPH-d histochemistry were corroborated by both the Nissl stain and CO histochemistry in adjacent sections (Fig. 5B and C).

The tangential distribution of NADPH-d neuropil in the barrel field is similar to the one described before (Pereira Jr. et al., 2000). In tangential sections, each NADPH-d barrel corresponded to a uniform stain of highly reactive neuropil flanked by regions of lightly labeled tissue (septa) (Pereira Jr. et al., 2000). The overall shape of barrels is markedly similar to that revealed by both CO and SDH (Wong-Riley and Welt, 1980; Wallace, 1987). It was possible to visualize all representations of body parts in the barrel field, such as the head, the trunk, and the fore- and hindpaws. The field representing the trunk was identified as a region of high NADPH-d activity, but its borders were not sharp and individual barrels could not be clearly discerned. The PMBSF was the most salient subdivision due to its peculiar organization in five rows and four straddlers (Wallace, 1987). Its barrels had the largest diameter and were less irregularly shaped than those found in other sub-areas (see Pereira Jr. et al., 2000 for details).

3.3. Laminar and tangential distribution of type I NADPH-d cells in the SI barrel field

In the sections submitted to NADPH-d/NOS double labeling, the majority of NADPH-d type I cells was double-stained for NOS (see examples in Fig. 5D). In these double-labeled sections, we did not see neurons stained only for NOS. Also, no double-labeled neuron was found in control sections where the primary antibody was substituted by normal serum. Type I neurons were unevenly distributed across SI layers (check Fig. 5A for a representative section). Qualitative inspection of some non-tangential sections revealed that most type I neurons are concentrated in infragranular layers. A few cells could be found in supragranular layers, especially in layers II and III. In layer IV, type I cells seemed even rarer than in supragranular

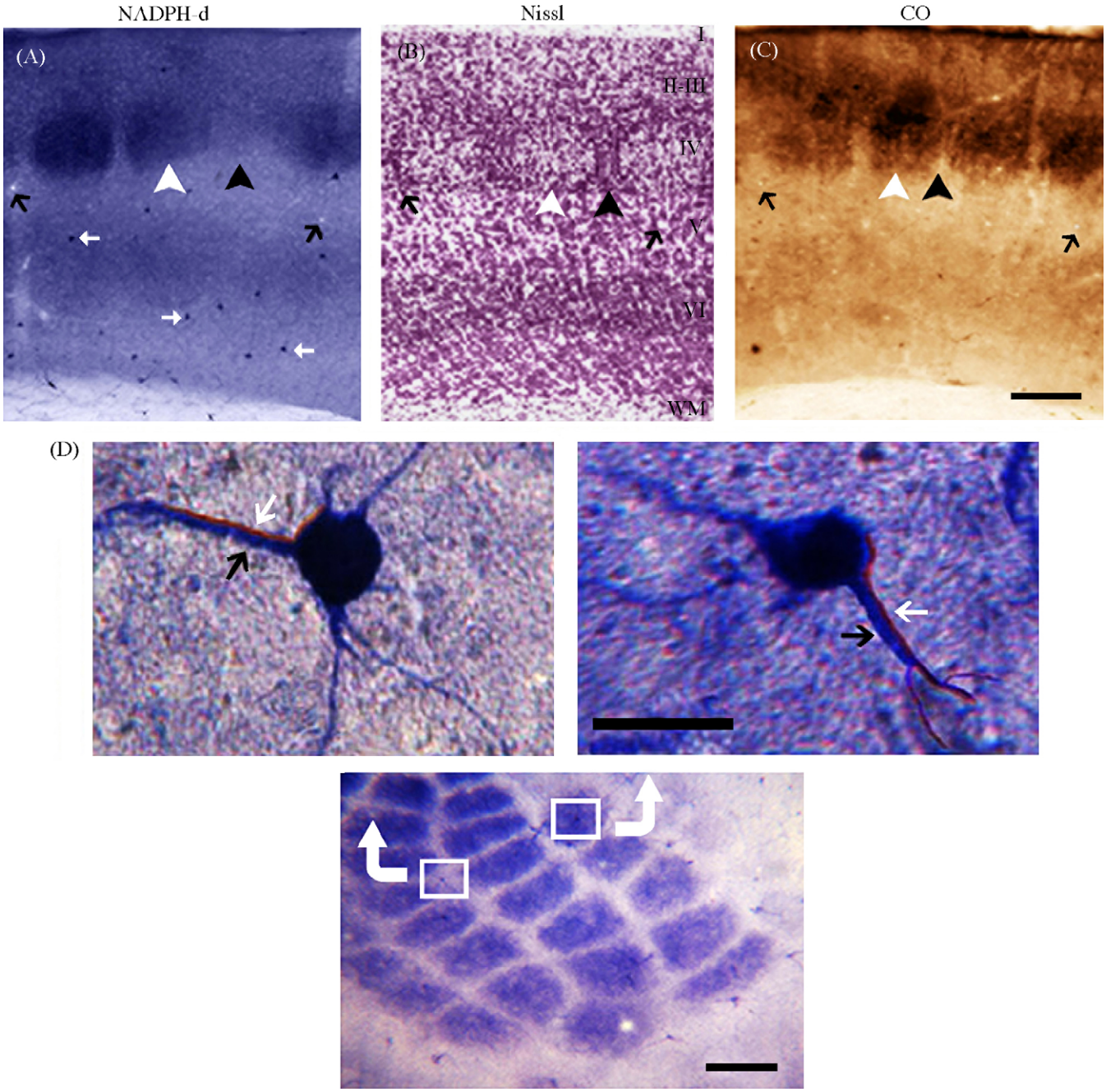

Fig. 5. Laminar distribution of NADPH-d and CO in the PMBSF. NADPH-d histochemistry revealed the complex layered architecture of the PMBSF, including the barrels in layer IV and a less prominent patchy distribution of neuropil reactivity in layer VI (A). Compare the NADPH-d distribution to the pattern provided by more classic methods like Nissl (B) and CO (C). Notice the higher number of type I cells located in the infragranular layers (A), some of them pointed by white arrows. Arrowheads in (A), (B) and (C) point to the same barrel (white) and septum (black) on adjacent sections (aligned with the help of blood vessels: small arrows). Type I cells in both barrels and septa were also double stained for NADPH-d (blue stain in (D), black arrows) and NOS immunohistochemistry (brown stain in (D), white arrows). Scale bars: 300 μm ((A)–(C) and lower part of (D)); 30 μm (enlargements of (D)).

layers, but their distribution was not homogeneous along the horizontal dimension: it was less likely to find a type I cell within a barrel's hollow than inside septa, a finding consistent with what has been previously described for neonate mice (Mitrovic and Schachner, 1996) and adult rats (Franca and Volchan, 1995; Freire et al., 2004). In the infragranular layers (V and VI), the number of type I cells increased when compared to any other layer (Fig. 5A), though without any obvious clustering, as in layer IV. Some cells were found scattered in the white matter, similar to what has been briefly described by Matsushita et al. (2001). Usually, the cell body of a NADPH-d neuron located in the

white matter was elongated in an axis parallel to the border with the gray matter, especially when located close to it (data not illustrated). This bias was also found in other species such as the rat (Freire et al., 2004) and the squirrel monkey (Franca et al., 1997).

On a tangential section through layer IV, it was easy to notice that, in the PMBSF, the number of type I neurons is higher in septa than in hollows (Fig. 6). This was quantitatively confirmed (septa: 50.4 ± 7.09; barrels: 19.6 ± 3.78, $p < 0.05$) (Fig. 7).

Type II neurons seemed to display a random distribution throughout SI and were commonly found in either supra or infragranular layers. We did not find type II cells in the white matter, a finding also reported for other mammalian species (Sandell, 1986; Franca et al., 1997, 2000; Freire et al., 2004). Due to both their weaker pattern of reactivity and susceptibility to increased levels of fixation (Sandell, 1986; Franca et al., 2000), type II cells were not quantified in this study.

4. Discussion

In the present work, we have analyzed the distribution and morphology of NADPH-d neurons in both tangential and coronal sections of the barrel cortex of adult mice. Our main results were fourfold. First, there was a clear segregation of type I cells in the PMBSF subcompartments, a result that is in disagreement with previous reports in younger animals (Mitrovic and Schachner, 1996). Second, type I neurons found in septal regions possess a more complex and exuberant dendritic field than those found inside barrels. Third, it was possible to discern a higher number of these cells located in infragranular layers as compared to granular and supragranular layers. Fourth, the strongly reactive neuropil in layer IV delineates barrel fields that are vertically aligned with weakly reactive barrel-like structures in layer VI. The significance of these findings will be discussed below.

4.1. NADPH-d type II neurons

Type II neurons have been found in the isocortex of many other mammalian species, from marsupials like the opossum (Franca et al., 2000) to both New- and Old-World primates (Sandell, 1986; Franca et al., 1997, 2000). In early reports, however, the presence of type II neurons in rodents ranged from being neglected to altogether dismissed (Mitrovic and Schachner, 1996; Yan and Garey, 1997; Oermann et al., 1999). Later, we were able to demonstrate that NADPH-d type II cells are unequivocally present in the rodent's brain (Pereira Jr. et al., 2000; Picanço-Diniz et al., 2004; Freire et al., 2004).

We suggest that the observed discrepancy might be explained, at least in part, by differences in the fixation procedures adopted on different studies. Since excessive fixation can abolish the development of the NADPH-d stain (Spessert and Layes, 1994; Franca et al., 2000), it is feasible that this procedure might have inhibited the proper staining of type II neurons in other studies (Sandell, 1986; see also Franca et al., 2000). Accordingly, in the present study we could barely identify type II neurons in more fixed tissue (data not shown).

4.2. Distribution of NADPH-d type I neurons and reactive neuropil

Type I cells tended to be more concentrated in septa than in the barrels proper, as previously reported for the adult rat (Valtschanoff et al., 1993; Franca and Volchan, 1995; Freire et al., 2004). This heterogeneous distribution pattern seems to be established early during the first postnatal week in mice (Mitrovic and Schachner, 1996) and, according to the present study, is maintained during adulthood.

During the course of the mouse postnatal development, there is a significant higher concentration of NADPH-d type I neurons in septa than inside barrels (Mitrovic and Schachner, 1996). However, it has also been reported that this difference, as well as the barrels themselves, completely disappears after 15 days of age (Mitrovic and Schachner, 1996; Oermann et al., 1999). Our present results, on the other hand, reveal not only a clearly delineated NADPH-d-reactive barrel field (see also Pereira Jr. et al., 2000) but also a significant higher concentration of type I neurons in the septal region of mature animals. The distribution of type I cells reported here for the mouse is in accordance with previous studies on the adult rat (Valtschanoff et al., 1993; Franca and Volchan, 1995; Freire et al., 2004).

The relative absence of type I neurons inside barrels does not necessarily imply that this cortical region synthesizes less nitric oxide than septa. We demonstrated that neuropil reactivity is remarkably elevated inside barrels. This reactive neuropil can be a source of nitric oxide as well. The actual origin of such NOS/NADPH-d-positive neuropil remains to be clarified. Most of the input to layer IV barrels is carried by axon terminals arriving from the ventral posteromedial thalamic nucleus (VPM) (Koralek et al., 1988; Lu and Lin, 1993), but this nucleus does not seem to contain many NADPH-d reactive cell bodies (Vincent and Kimura, 1992; Kharazia et al., 1997; Simpson et al., 2003). Similarly, in layer IVC of the monkey's visual cortex, there is also a high concentration of dispersed NOS/NADPH-d neuropil but few reactive cellular profiles (Franca et al., 1997). Using electron microscopy reconstructions, Aoki et al. (1993) have demonstrated that this NOS-immunoreactive neuropil corresponds predominantly to presynaptic terminals whose origin is still unknown.

Another interesting finding is the presence of barrel-like structures located in layer VI and which are in register with the more reactive barrels in the overlying layer IV. During the postnatal development of the somatosensory cortex, NO activity in layers V and VI is detected earlier than activity in layer IV, being more intense during the first postnatal week

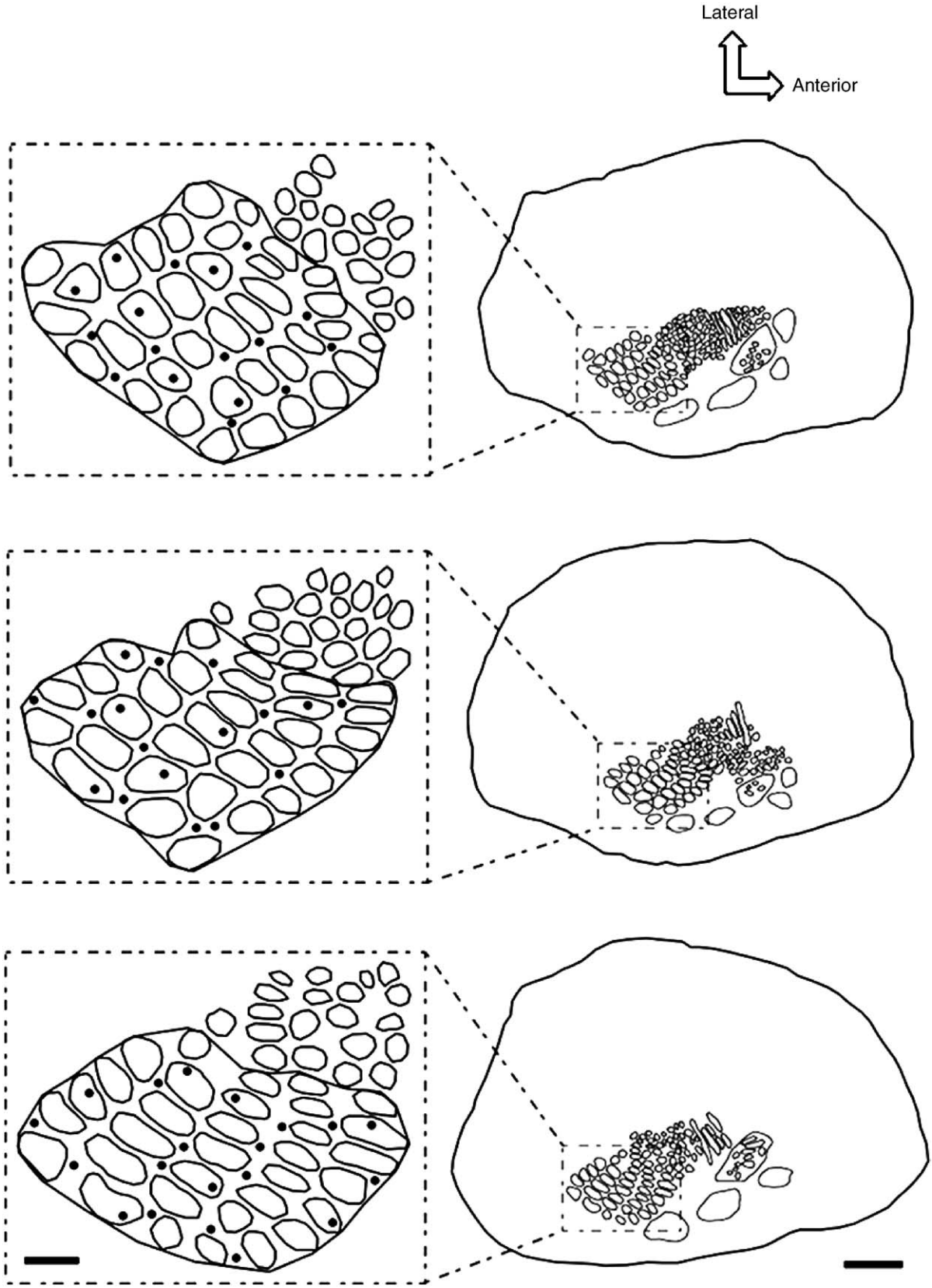

Fig. 6. Tangential distribution of layer IV type I NADPH-d neurons in the PMBSF. Tangential reconstructions of all barrel fields from three different cases are depicted in the right column. At the left-side, the enlargements show the delimitation of the PMBSF, where areal measurements were performed. Black dots represent type I NADPH-d cells in both septa and barrel hollows. Notice that type I cells are more common in septa than inside barrels. Scale bars: 2 mm; 300 μm (enlargements).

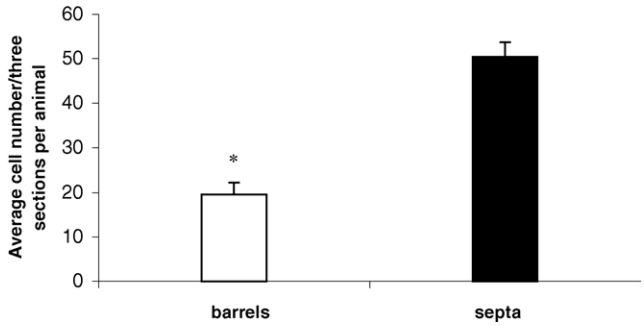

Fig. 7. Distribution of type I NADPH-d-stained cells in PMBSF's sub-compartments. The number of NADPH-d cells in septa was always higher than inside barrels ($^{*}p < 0.05$; Student's *t*-test).

(Imura et al., 2005). Only later, at P10, this activity extends to layer IV (Imura et al., 2005). Imura et al. (2005) speculate that the presence of NO during this period might be crucial for synapse formation. Our findings that type I neurons are not only more concentrated in infragranular layers but that neuropil reactivity, though not as robust as in layer IV, is nonetheless strong in layer VI suggest that this pattern is maintained in adulthood. The origin of NADPH-d neuropil reactivity in layer VI remains to be determined. In the rat, most of the terminals arriving in layer VI come from the neighboring motor cortex (Zhang and Deschênes, 1998).

Layer VI is considered the principal source of feedback projections to the somatosensory thalamus, forming a loop responsible for the modulation of thalamic responses to peripheral stimuli (see Ghazanfar et al., 2001). Regions of layer VI directly below the barrels project exclusively to the VPM, whilst regions below septa project both to the VPM and to the posterior medial nucleus (POm) (Killackey and Sherman, 2003). Thus, the modular architecture revealed by NADPH-d in layer VI should be related to segregated circuits in these different zones. Such circuits originate different corticothalamic outputs from barrel and septal columns, corroborating the idea that the septa are in fact a different kind of cortical tissue (possibly a higher order cortex) intermingled with the actual primary somatosensory cortex (i.e. the barrels themselves; see Killackey and Sherman, 2003). Morphological differences between layer IV's type I neurons found in barrel versus septal regions further reinforce this point, as discussed below.

4.3. Morphometry of type I neurons

The morphology of type I NADPH-d neurons in the PMBSF is not homogeneous. Cells can be subdivided into two groups, depending whether they are localized in septa or barrels. Three morphometric parameters were measured for NADPH-d cells: cell body area, dendritic field area, and fractal dimension.

There was no significant difference between the areas of neuronal cell bodies found either in septa and barrels. The dendritic field area of neurons found in septal regions, on the other hand, is significantly higher than barrels' cells. In addition, the fractal dimension values (*D*) of cells in these two subregions were found to differ markedly, reflecting significant dissimilarities in their dendritic arborizations, with septal neurons having more complex dendritic fields. The fractal dimension has been demonstrated before to be an useful parameter to characterize morphological differences among cell sub-groups (Porter et al., 1991; Jelinek and Elston, 2001, 2003).

The larger dendritic coverage of septal neurons should be related to the distinct physiological properties of these two regions (see Kim and Ebner, 1999). Similar to what was discussed in the previous section, the ascending thalamic projection to septa and barrels is also segregated. Septa receive their main thalamic input from the POm, while the input to barrels comes from the VPM (Lu and Lin, 1993). Also, callosal terminals originating from the contralateral primary somatosensory cortex are mainly localized in septa (Hayama and Ogawa, 1997). The morphometric differences between neurons located in these two zones of layer IV provides further support to the notion of two parallel streams for the processing of tactile information, one passing through the barrels and the other through the septa. It is possible that NADPH-d neurons with different types of axonal arbors are part of specialized inhibitory circuits customized for each of these two subregions, since inhibitory cortical neurons contribute for a thalamus-evoked feedforward inhibition in the mouse barrel cortex (Porter et al., 2001).

In conclusion, the presence of both cellular and neuropil reactivity for NADPH-d in the adult barrel field is evidence that NO should play an important role in the adult somatosensory system, possibly involved with functions such as the processing of sensory information (Kara and Friedlander, 1999), control of cerebral blood flow (Iadecola, 1993), and/or regulation of neuronal metabolism (Wong-Riley et al., 1998). In addition, differences in the cellular morphology of NADPH-d type I neurons in the barrel field subcompartments is likely to be related to fine aspects of specific neuronal circuits in these structures. Future studies are needed in order to evaluate the functional implications of both the uneven distribution of NADPH-d neuropil and the distinct morphology of type I neurons in the rodent barrel field.

Acknowledgments

The authors wish to thank Dr. Sidarta Ribeiro for his comments on an earlier version of the manuscript. This study was part of the requirements for the PhD's degree of Marco Aurelio M. Freire by the UFPA's Biological Sciences Building. Research supported by grants from Conselho Nacional de Desenvolvimento Científico e Tecnológico (CNPq), and Programa de Apoio a Núcleos de Excelência (PRONEX), Brazil.

References

Aoki, C., Fenstermaker, S., Lubin, M., Go, G.G., 1993. Nitric oxide synthase in the visual cortex of monocular monkeys as revealed by light and electron microscopic immunocytochemistry. Brain Res. 620, 97–113.

Bidmon, H.J., Wu, J., Gödecke, A., Schleicher, A., Mayer, B., Zilles, K., 1997. Nitric oxide synthase expressing neurons are area-specifically distributed within the cerebral cortex of the rat. Neuroscience 81, 321–330.

Bohme, G.A., Bon, C., Stutzman, J.M., Doble, A., Blanchard, J.C., 1991. Possible involvement of nitric oxide in long term potentiation. Eur. J. Pharmacol. 199, 379–381.

Caserta, F., Eldred, W.D., Fernandez, E., Hausman, R.E., Stanford, L.R., Bulderev, S.V., Schwarzer, S., Stanley, H.E., 1995. Determination of fractal dimension of physiologically characterized neurons in two and three dimensions. J. Neurosci. Meth. 56, 133–144.

Dawson, T.M., Bredt, D.S., Fotuhi, M., Hwang, P.M., Snyder, S.H., 1991. Nitric oxide synthase and neuronal NADPH diaphorase are identical in brain and peripheral tissues. Proc. Natl. Acad. Sci. U.S.A. 88, 7797–7801.

DeFelipe, J., 1997. Types of neurons, synaptic connections and chemical characteristics of cells immunoreactive for calbindin-D28K, parvalbumin and calretinin in the neocortex. J. Chem. Neuroanat. 14, 1–19.

Ernst, A.F., Wu, H.H., El-Fakahany, E.E., Mcloon, S.C., 1999. NMDA receptor-mediated refinement of a retinotectal projection during development requires nitric oxide. J. Neurosci. 19, 229–235.

Estevez, A.G., Spear, N., Manuel, S.M., Radi, R., Henderson, C.E., Barbeito, L., Beckman, J.S., 1998. Nitric oxide and superoxide contribute to motor neuron apoptosis induced by trophic factor deprivation. J. Neurosci. 18, 923–931.

Estrada, C., DeFelipe, J., 1998. Nitric oxide-neurons in the neocortex, morphological and functional relationship with intraparenchimal microvasculature. Cereb. Cortex 8, 193–203.

Ferrante, R.J., Kowall, N.W., Beal, M.F., Richardson Jr., E.P., Bird, E.D., Martin, J.B., 1985. Selective sparing of a class of striatal neurons in Huntington's disease. Science 230, 561–563.

Franca, J.G., 1999. NADPH-diaphorase in the mammalian isocortex: type I neurons and reactive neuropil in visual and somatosensory cortices. Doctor in Science's Thesis. Federal University of Rio de Janeiro, Brazil, 145 pp. (in Portuguese).

Franca, J.G., Volchan, E., 1995. NADPH diaphorase histochemistry as a marker for barrels in rat somatosensory cortex. Braz. J. Med. Biol. Res. 28, 787–790.

Franca, J.G., Volchan, E., Jain, N., Catania, K.C., Oliveira, R.S.L., Hess, F.F., Jablonka, M., Rocha-Miranda, C.E., Kaas, J.H., 2000. Distribution of NADPH diaphorase cells in visual and somatosensory cortex in four mammalian species. Brain Res. 864, 163–175.

Franca, J.G., Do-Nascimento, J.L.M., Picanço-Diniz, C.W., Quaresma, J.A.S., Silva, A.L.C., 1997. NADPH-diaphorase activity in area 17 of the squirrel monkey visual cortex, neuropil pattern, cell morphology and laminar distribution. Braz. J. Med. Biol. Res. 30, 1093–1105.

Freire, M.A.M., Gomes-Leal, W., Carvalho, W.A., Guimarães, J.S., Franca, J.G., Picanço-Diniz, C.W., Pereira Jr., A., 2004. A morphometric study of the progressive changes on NADPH diaphorase activity in the developing rat's barrel field. Neurosci. Res. 50, 55–66.

Ghazanfar, A.A., Krupa, D.J., Nicolelis, M.A.L., 2001. Role of cortical feedback in the receptive field structure and nonlinear response properties of somatosensory thalamic neurons. Exp. Brain Res. 141, 88–100.

Hashikawa, T., Leggio, M.G., Hattoric, R., Yui, Y., 1994. Nitric oxide synthase immunoreactivity colocalized with NADPH-diaphorase histochemistry in monkey cerebral cortex. Brain Res. 641, 341–349.

Hayama, T., Ogawa, H., 1997. Regional differences of callosal connections in the granular zones of the primary somatosensory cortex in rats. Brain Res. Bull. 43, 341–347.

Hölscher, C., 1997. Nitric oxide, the enigmatic neuronal messenger, its role in synaptic plasticity. Trends Neurosci. 20, 298–303.

Hope, B.T., Michael, G.J., Knigge, K.M., Vincent, S.R., 1991. Neuronal NADPH diaphorase is a nitric oxide synthase. Proc. Natl. Acad. Sci. U.S.A. 88, 2811–2814.

Iadecola, C., 1993. Regulation of the cerebral microcirculation during neural activity: is nitric oxide the missing link? Trends Neurosci. 16, 206–214.

Imura, T., Kanatani, S., Fukuda, S., Miyamoto, Y., Hisatsune, T., 2005. Layer-specific production of nitric oxide during cortical circuit formation in postnatal mouse brain. Cereb. Cortex 15, 332–340.

Jelinek, H.F., Elston, G.N., 2001. Pyramidal neurones in macaque visual cortex: interareal phenotypic variation of drendritic branching patterns. Fractals 3, 287–295.

Jelinek, H.F., Elston, G.N., 2003. Dendritic branching of pyramidal cells in the visual cortex of the nocturnal owl monkey: a fractal analysis. Fractals 4, 391–396.

Jelinek, H.F., Fernandez, E., 1998. Neurons and fractals: how reliable and useful are calculations of fractal dimensions? J. Neurosci. Meth. 81, 9–18.

Jelinek, H.F., Fernandez, E., 2001. Use of fractal theory in neuroscience: methods, advantages, and potential problems. Methods 24, 309–321.

Kalb, R.G., Agostini, J., 1993. Molecular evidence for nitric oxide-mediated motor neuron development. Neuroscience 57, 1–8.

Kara, P., Friedlander, M.J., 1999. Arginine analogs modify signal detection by neurons in the visual cortex. J. Neurosci. 19, 5528–5548.

Kharazia, V.N., Petrusz, P., Usunoff, K., Weinberg, R.J., Rustioni, A., 1997. Arginine and NADPH diaphorase in the rat ventroposterior thalamic nucleus. Brain Res. 744, 151–155.

Killackey, H.P., Sherman, S.M., 2003. Corticothalamic projections from the rat primary somatosensory cortex. J. Neurosci. 23, 7381–7384.

Kim, U., Ebner, F.F., 1999. Barrels and septa, separate circuits in rat barrels field cortex. J. Comp. Neurol. 408, 489–505.

Koh, J.Y., Peters, S., Choi, D.W., 1986. Neurons containing NADPH-diaphorase are selectively resistant to quinolinate toxicity. Science 234, 73–76.

Koralek, K.A., Jensen, K.F., Killackey, H.P., 1988. Evidence for two complementary patterns of thalamic input to the rat somatosensory cortex. Brain Res. 463, 346–351.

Kubota, Y., Kawaguchi, Y., 1994. Three classes of GABAergic interneurons in neocortex and neostriatum. Jpn. J. Physiol. 44, S145–S148.

Lipton, S.A., Choi, Y.B., Pan, Z.H., Lei, S.Z., Chen, S.H., Sucher, N.J., Losalzo, J., Singel, D.J., Stamler, J.S., 1993. A redox-based mechanism for neuroprotective and neurodestructive effects of nitric oxide and related-nitroso compounds. Nature 364, 626–632.

Lorente de Nó, R., 1992. The cerebral cortex of the mouse (a first contribution—the "acoustic" cortex). Somatosens. Mot. Res. 9, 3–36 (English translation of the Spanish original 1922 article, translated by Fairén, A., Regidor, J., and Kruger, L.)

Lu, S.M., Lin, R.C.-S., 1993. Thalamic afferents of the rat barrel cortex: a light and electron-microscopy study using *Phaseolus vulgaris* leucoagglutinin as an anterograde tracer. Somatosens. Mot. Res. 10, 1–16.

Lüth, H.-J., Hedlich, A., Heidegard, H., Winkelmann, E., Mayer, B., 1994. Morphological analyses of NADPH-diaphorase/nitric oxide synthase positive structures in human visual cortex. J. Neurocytol. 23, 770–782.

Matsushita, H., Takeuchi, Y., Mitsuhiro, K., Sawada, T., 2001. Distribution of NADPH-diaphorase positive neurons in the mouse brain, differences from previous findings in the rat brain and comparison with the distribution of serotonergic neurons. Acta Histochem. Cytochem. 34, 235–257.

Mitrovic, N., Schachner, M., 1996. Transient expression of NADPH diaphorase activity in the mouse whisker to barrel field pathway. J. Neurocytol. 25, 429–437.

Moreno-Lopez, B., Noval, J.A., González-Bonet, L.G., Estrada, C., 2000. Morphological bases for a role of nitric oxide in adult neurogenesis. Brain Res. 869, 244–250.

Nelson, R.J., Demas, G.E., Huang, P.L., Fishman, M.C., Dawson, V.L., Dawson, T.M., Snyder, S.H., 1995. Behavioral abnormalities in male mice lacking neuronal nitric oxide synthase. Nature 378, 383–386.

Oermann, E., Bidmon, H.J., Mayer, B., Zilles, K., 1999. Differential maturation of nitric oxide synthase-I and NADPH diaphorase in functionally distinct cortical areas of the mouse cerebral cortex. Anat. Embryol. 200, 27–41.

Oliveira, R.B., Gomes-Leal, W., Do-Nascimento, J.L.M., Picanço-Diniz, C.W., 1998. Methylmercury intoxication and histochemical demonstration of NADPH diaphorase activity in the striate cortex of adult cats. Braz. J. Med. Biol. Res. 31, 1157–1161.

Pereira Jr., A., Freire, M.A.M., Pacheco-Bahia, C., Franca, J.G., Picanço-Diniz, C.W., 2000. The barrel field of the adult mouse SmI cortex as revealed by NADPH diaphorase histochemistry. Neuroreport 11, 1889–1892.

Picanço-Diniz, C.W., Araújo, M.R., Borba, J.M.C., Guedes, R.C.A., 1998. NADPH-diaforase containing neurons and biocytin-labelled axon terminals in the visual cortex of adult rats malnourished during development. Nutr. Neurosci. 1, 35–48.

Picanço-Diniz, C.W., Boche, D., Gomes-Leal, W., Perry, V.H., Cunningham, C., 2004. Neuropil and neuronal changes in hippocampal NADPH-diaphorase histochemistry in the ME7 model of murine prion disease. Neuropathol. Appl. Neurobiol. 30, 292–303.

Porter, R., Ghosh, S., David-Lange, G., Smith Jr., T.G., 1991. A fractal analysis of pyramidal neurons in mammalian motor cortex. Neurosci. Lett. 130, 112–116.

Porter, J.T., Johnson, C.K., Agmon, A., 2001. Diverse types of interneurons generate thalamus-evoked feedforward inhibition in the mouse barrel cortex. J. Neurosci. 21, 2699–2710.

Rice, F.L., 1995. Comparative aspects of barrel structure and development. In: Jones, E.G., Diamond, I.T. (Eds.), Cerebral Cortex, vol. 11: The Barrel Cortex of Rodents. Plenum Press, New York, pp. 1–75.

Riddle, D., Richards, A., Zsuppan, F., Purves, D., 1992. Growth of the rat somatic sensory cortex and its constituent parts during postnatal development. J. Neurosci. 12, 3509–3524.

Sandell, J.H., 1986. NADPH diaphorase histochemistry in the macaque striate cortex. J. Comp. Neurol. 251, 388–397.

Scherer-Singler, V., Vincent, S.R., Kimura, H., Mcgeer, F.G., 1983. Demonstration of a unique population of neurons with NADPH diaphorase histochemistry. J. Neurosci. Meth. 9, 229–234.

Shu, S., Ju, G., Fan, L., 1988. The glucose oxidase-DAB-nickel method in peroxidase histochemistry of the nervous system. Neurosci. Lett. 85, 169–171.

Simpson, K.L., Waterhouse, B.D., Lin, R.C., 2003. Differential expression of nitric oxide in serotonergic projection neurons: neurochemical identification of dorsal raphe inputs to rodent trigeminal somatosensory targets. J. Comp. Neurol. 466, 495–512.

Spessert, R., Layes, E., 1994. Fixation conditions affect the intensity but not the pattern of NADPH-diaphorase staining as a marker for neuronal nitric oxide synthase in rat olfactory bulb. J. Histochem. Cytochem. 42, 1309–1315.

Tanaka, M., Yoshida, S., Yano, M., Hanaoka, F., 1994. Roles of endogenous nitric oxide in cerebellar cortical development in slice cultures. Neuroreport 5, 2049–2052.

Thomas, E., Pearse, A.G.E., 1964. The solitary active cells. Histochemical demonstration of damage-resistant nerve cells with a TPN-diaphorase reaction. Acta Neuropathol. 3, 238–249.

Valtschanoff, J.G., Weinberg, R.J., Kharazia, V.N., Schmidt, H.H.H.W., Nakane, M., Rustioni, A., 1993. Neurons in rat cerebral cortex that synthesize nitric oxide: NADPH diaphorase histochemistry, NOS immunocytochemistry, and colocalization with GABA. Neurosci. Lett. 157, 157–161.

van der Loos, H., Woolsey, T.A., 1973. Somatosensory cortex: structural alterations following early injury to sensory organs. Science 179, 395–398.

Vincent, S.R., 1994. Nitric oxide, a radical neurotransmitter in the central nervous system. Prog. Neurobiol. 42, 129–160.

Vincent, S.R., Kimura, H., 1992. Histochemical mapping of nitric oxide synthase in the rat brain. Neuroscience 46, 755–784.

Volchan, E., Franca, J.G., 1994. Distribution of NADPH-diaphorase-positive neurons in the opossum neocortex. Braz. J. Med. Biol. Res. 27, 2431–2435.

Wallace, M.N., 1987. Histochemical demonstration of sensory maps in the rat and mouse cerebral cortex. Brain Res. 418, 178–182.

Welker, C., Woolsey, T.A., 1974. Structure of layer IV in the somatosensory neocortex of the rat description and comparison with the mouse. J. Comp. Neurol. 158, 437–454.

Weller, W.L., 1993. SmI cortical barrels in an Australian marsupial, *Trichosurus vulpecula* (brush tailed possum): structural organization, patterned distribution, and somatotopic relationships. J. Comp. Neurol. 337, 471–492.

Wong-Riley, M.T.T., 1979. Changes in the visual system of monocularly sutured or enucleated cats demonstrable with cytochrome oxidase histochemistry. Brain Res. 171, 11–28.

Wong-Riley, M.T.T., Anderson, B., Liebl, W., Huang, Z., 1998. Neurochemical organization of the macaque striate cortex: correlation of cytochrome oxidase with Na(+)K(+)ATPase, NADPH-diaphorase, nitric oxide synthase, and *N*-methyl-D-aspartate receptor subunit 1. Neuroscience 83, 1025–1045.

Wong-Riley, M.T.T., Welt, C., 1980. Histochemical changes in cytochrome oxidase of cortical barrel of the vibrissal removal in neonatal and adult mice. Proc. Natl. Acad. Sci. U.S.A. 77, 2333–2337.

Woolsey, T.A., van der Loos, H., 1970. The structural organization of layer IV in the somatosensory region (SI) of mouse cerebral cortex: the description of a cortical field composed of discrete cytoarchitectonic units. Brain Res. 17, 205–242.

Woolsey, T.A., Welker, C., Schwartz, R.H., 1975. Comparative anatomical studies of the SmI face cortex with special reference to the occurrence of "barrels" in layer IV. J. Comp. Neurol. 164, 79–94.

Yan, X.X., Garey, L.J., 1997. Morphological diversity of nitric oxide synthesising neurons in mammalian cerebral cortex. J. Brain Res. 38, 165–172.

Yan, X.X., Jen, L.S., Garey, L.J., 1996. NADPH-diaphorase positive neurons in primate cerebral cortex colocalize with GABA and calcium-binding proteins. Cereb. Cortex 6, 524–529.

Zhang, Z.W., Deschênes, M., 1998. Projections to layer VI of the posteromedial barrel field in the rat: a reappraisal of the role of corticothalamic pathways. Cereb. Cortex 8, 428–436.

Zilles, K., Wree, A., 1985. Cortex, areal and laminar structure. In: Paxinos, G. (Ed.), Forebrain and Midbrain. Academic Press/Harcourt Brace Jovanovic, New York, pp. 375–415.